Double Rabi Splitting in a Strongly Coupled System of Core–Shell Au@Ag Nanorods and J-Aggregates of Multiple Fluorophores

Dzmitry Melnikau, Alexander Govyadinov, Ana Sánchez-Iglesias, Marek Grzelczak, Igor Nabiev, Luis Liz-Marzán, Yury Rakovich

Double Rabi splitting in a strongly coupled system of core-shell Au@Ag nanorods and J-aggregates of multiple fluorophores

Dzmitry Melnikau[1,2], Alexander A. Govyadinov[3], Ana Sánchez-Iglesia[4], Marek Grzelczak[5,6], Igor R. Nabiev[7,8], Luis M. Liz-Marzán[4,6,8], Yury P. Rakovich[5,6,8,10]

[1]CIC NanoGUNE, Ave. Tolosa 76, 20018 Donostia-San Sebastian, Spain

[2]National University of Ireland Galway, University Road, H91 TK33, Galway, Ireland

[3]neaspec GmbH, Eglfinger Weg 2, Haar, 85540, Germany

[4]CIC biomaGune, Paseo de Miramón 182, 20014 Donostia-San Sebastian, Spain

[5]Donostia International Physics Center (DIPC), Paseo Manuel de Lardizabal 4, 20018 Donostia-San Sebastian, Spain

[6]IKERBASQUE, Basque Foundation for Science, Maria Diaz de Haro 3, 48013 Bilbao, Spain

[7]Laboratoire de Recherche en Nanosciences, LRN-EA4682, Université de Reims Champagne-Ardenne, 51100 Reims, France

[8]National Research Nuclear University MEPhI (Moscow Engineering Physics Institute), 115409 Moscow, Russian Federation

[9]Biomedical Research Networking Center in Bioengineering Biomaterials and Nanomedicine, Ciber-BBN, Paseo de Miramón 182, 20014 Donostia-San Sebastián, Spain

[10]Centro de Física de Materiales (MPC, CSIC-UPV/EHU) and Departamento de Física de Materiales UPV-EHU, Paseo Manuel de Lardizabal 5, 20018 Donostia-San Sebastian, Spain

AUTHOR INFORMATION

Corresponding Author

*Yury.Rakovich@ehu.eus

ABSTRACT The interaction of several components in the strong coupling regime yielding multiple Rabi splittings opens up remarkable possibilities for studies of

multimode hybridization and energy transfer, which is of considerable interest in both fundamental and applied science. Here we demonstrate that three different components such as core-shell Au@Ag nanorods and J-aggregates of two different dyes, can be integrated into a single hybrid structure, which leads to strong collective exciton-plasmon coupling and double-mode Rabi splitting totaling 338 meV. We demonstrate strong coupling in these multicomponent plexitonic nanostructures by means of magnetic circular dichroism spectroscopy, and demonstrate strong magneto-optical activity for the three hybridized states resulting from this coupling. The J-aggregates of two different non-magnetic dyes interact with metal nanoparticles effectively, achieving magnetic properties due to the hybridization of electronic excitations in the three-component system.

TOC GRAPHICS

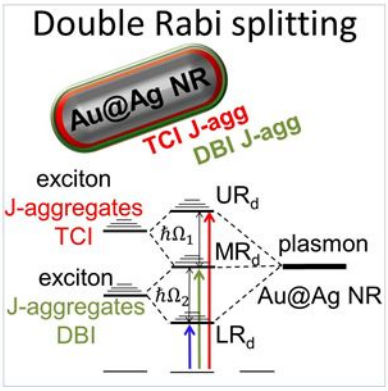

KEYWORDS Strong coupling, double Rabi splitting, J-aggregates, plexciton, magneto-optical activity, magnetic circular dichroism.

The interaction of organic and inorganic materials in a strong coupling regime significantly changes the characteristics of the individual components, yielding a hybrid system with new physical and chemical properties. It has been recently demonstrated that strong coupling can affect the rate of chemical reactions [1], pathways of energy- and electron- transfer [2-3], fluorescence [4-5], conductivity [6] and magnetic properties [7] of integrated materials.

The strong coupling regime is achieved when the rate of coherent energy exchange between excitons and plasmons exceeds the dissipation rate in the plexcitonic system [8]. This leads to the formation of new hybrid plexciton states (which causes spectral Rabbi splitting) with remarkable mixed properties in the assembled materials, thereby providing new opportunities for various

applications in the fields of information processing [9-11], sensing [7] and being at the core of plasmonic switches based on the strong coupling effect [12].

Apart from "classical" double-component strongly coupled systems, another direction with significant untapped potential in the field of light-matter interactions is the study of strongly coupled multicomponent systems. The emergence of multiple Rabi splitting in such systems is of considerable interest and relevance for both fundamental and applied science, providing remarkable opportunities for studies of multimode hybridization and energy transfer [2, 13-16]. Moreover, multimode strong coupling can open the way to multipartite entanglement and the implementation of quantum computing devices using multi-quasiparticle boson systems [17-18].

The development of strongly coupled multicomponent systems, namely two J-aggregated cyanine dyes incorporated in a microcavity, have led to the discovery of an efficient and ultrafast pathway for the energy-transfer between two exciton states [2]. Multiple spectral splittings for molecular vibrations coupled with a set of infrared cavity modes have also been reported [15]. Despite the fact that plasmon nanostructures (*i.e.* nanoresonators) are considered to be an alternative to microcavities for achieving a strong coupling regime [19], so far there are no convincing reports on multiple Rabi splittings in coupled exciton-plasmon systems. In the only work we have found on this topic, double Rabi splitting was

observed in the extinction spectra of a complex system comprising gold nanostars and J-aggregates of two dyes [16]. However, the strong interaction of the fluorophores with plasmonic nanostructures was not convincingly demonstrated. Also we would like to note that recently double Rabi splitting was observed in dark- field scattering spectra using a plasmonic nanostructure interacting with two types of excitons (charged and neutral) in WS_2 with decreasing temperature [20].

Here we unambiguously show that strong collective coupling can be reached in a system made of Au@Ag nanorods (NRs) and J-aggregates of two different dyes, which form a single nanosystem with unique multiple spectral features. We demonstrate magneto-optical activity for three hybridized plexciton states resulting from strong exciton-plasmon coupling in multilayer nanostructures, in which the plasmonic component induces magnetic properties in non-magnetic organic fluorophores. Our findings are of significance for the development of new sensing systems based on magneto-optical activity, while significantly expanding the portfolio of materials that can be used for information storage and processing.

The extinction spectra of J-aggregates of 5,5′,6,6′-Tetrachloro-1,1′,3,3′-tetraethyl-imidacarbocyanine iodide (TCI) and 2-[3-[1,1-dimethyl-3-(4-sulfobutyl)-1,3-dihydro-benzo[e]indol-2-ylidene]-propenyl]-1,1-dimethyl-3-(4-sulfobutyl)-1H-benzo[e]indolium hydroxide (DBI) dyes show narrow peaks (so called J-bands) red-shifted with respect to the respective monomer peaks (Figure 1a). Formation of J-bands and associated spectral shift upon aggregation of monomers is

caused by the delocalization and migration of the exciton energy over a large number of aggregated dye molecules [21]. The absorption maxima of J-bands are observed at 587 nm and 637 nm, with a full-width at half-maximum of 24.4 and 20 nm for TCI and DBI dyes, respectively.

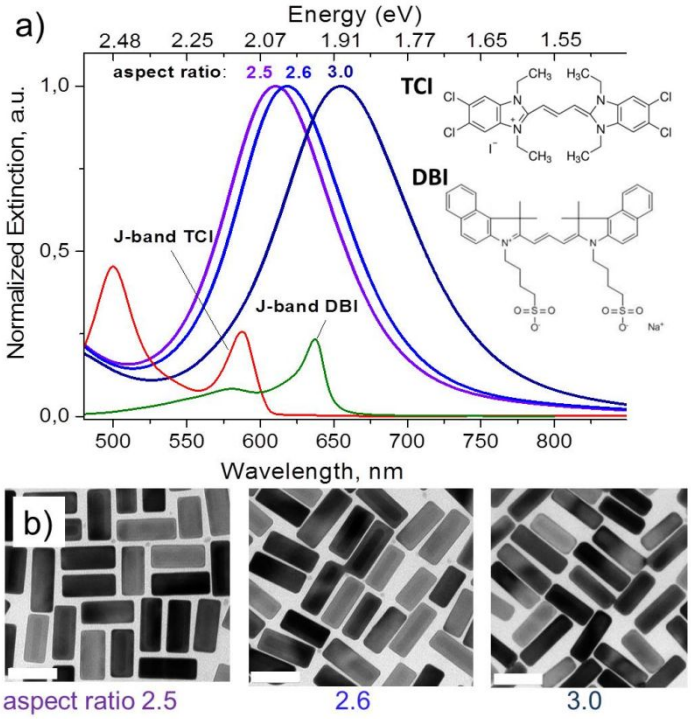

Figure 1. (a) Experimental extinction spectra of an aqueous dispersion of core-shell Au@Ag NRs of different aspect ratios (2.5 – 3.0) and absorption spectra of J-aggregates of TCI and DBI fluorophores (inset: chemical structures of TCI and DBI fluorophores). (b) TEM images of core-shell Au@Ag NRs with average aspect ratios varying from 2.5 to 3; scale bars are 50 nm.

The synthesized Au@Ag NRs have rather wide plasmon resonance bands (200-300 eV) corresponding to the longitudinal modes, which are located in the spectral region of J-bands of TCI and DBI dyes (Figure 1a). We would like to note, that the width of plasmon peaks observed in our case in the spectra of ensembles of nanorods is dominated by the inhomogeneous broadening due to the dispersion of the of nanorods. As reported in previous studies, typical linewidths for single nanorods with the aspect ratios close to that of our samples were found to be, for example, 23-83 [22], 75 [23] and 68 meV [24].

In contrast to our previous work [4], in the present experiments we control the spectral position of the longitudinal surface plasmon resonance in the samples, not by changing the NR length but by varying the thickness of the Ag shell deposited on the Au NR core. Increasing the thickness of the Ag layer, which is known to preferentially grow on the sides of the Au NRs [25], the aspect ratio (AR, the ratio of length-to-width of NR) was varied from 3 to 2.5 (Figure 1a). Such an AR modification leads in turn to a shift of the longitudinal LSPR, from 655 nm to 610 nm (Figure 1a). Thus, an ideal overlap of the localized surface plasmon resonance (LSPR) band with the spectral position of the J-bands of both dyes can be ensured, providing the best conditions for a strong exciton-plasmon interaction in the developed nanostructures.

The double Rabi splitting in the extinction spectra of the hybrid structures was achieved as a result of the sequential assembly of TCI J-aggregates on Au@Ag

NRs, followed by deposition of DBI J-aggregates. The interaction of two oppositely charged fluorophores stimulated the formation of a hybrid system comprising Au@Ag NRs coated with two layers of different J-aggregate dyes. It is also important to note that any attempt to create a separate hybrid system of bare Au@Ag NR and J-aggregates of DBI fluorophore, possessing strong coupling properties, was not successful. This is likely related to the efficient interaction of DBI dye with free (non-bound to NR surface) surfactant (benzyldimethylhexadecylammonium chloride, BDAC), which seems to be only weakly bound to the surface of the plasmon particle, thereby preventing efficient plasmon-exciton coupling. Interaction of DBI dye with BDAC was assumed on the basis that the positively charged polyelectrolytes, i.e. BDAC, hexadecyltrimethylammonium bromide (CTAB), poly(diallyldimethylammonium) chloride (PDDA) or polyethyleneimine (PEI), can trigger the formation of DBI dye aggregates.

In the extinction spectra of TCI/Au@Ag nanostructures, strong coupling effects manifest themselves as a pronounced dip in the region of the J-band (590-595 nm) with two plexciton peaks, associated to so-called upper (URs) and lower (LRs) resonances (indicated by arrows in Figure 2a). With an increase in the AR, a shift of both resonances is observed: the UR approaches the spectral position of the J-band, while the LR moves away from the absorption band of the excitons.

Figure 2 shows that, for NRs with all considered AR, the LRs in the spectra of hybrid NRs/TCI J-aggregates structures strongly overlap with the J-band of the DBI dye.

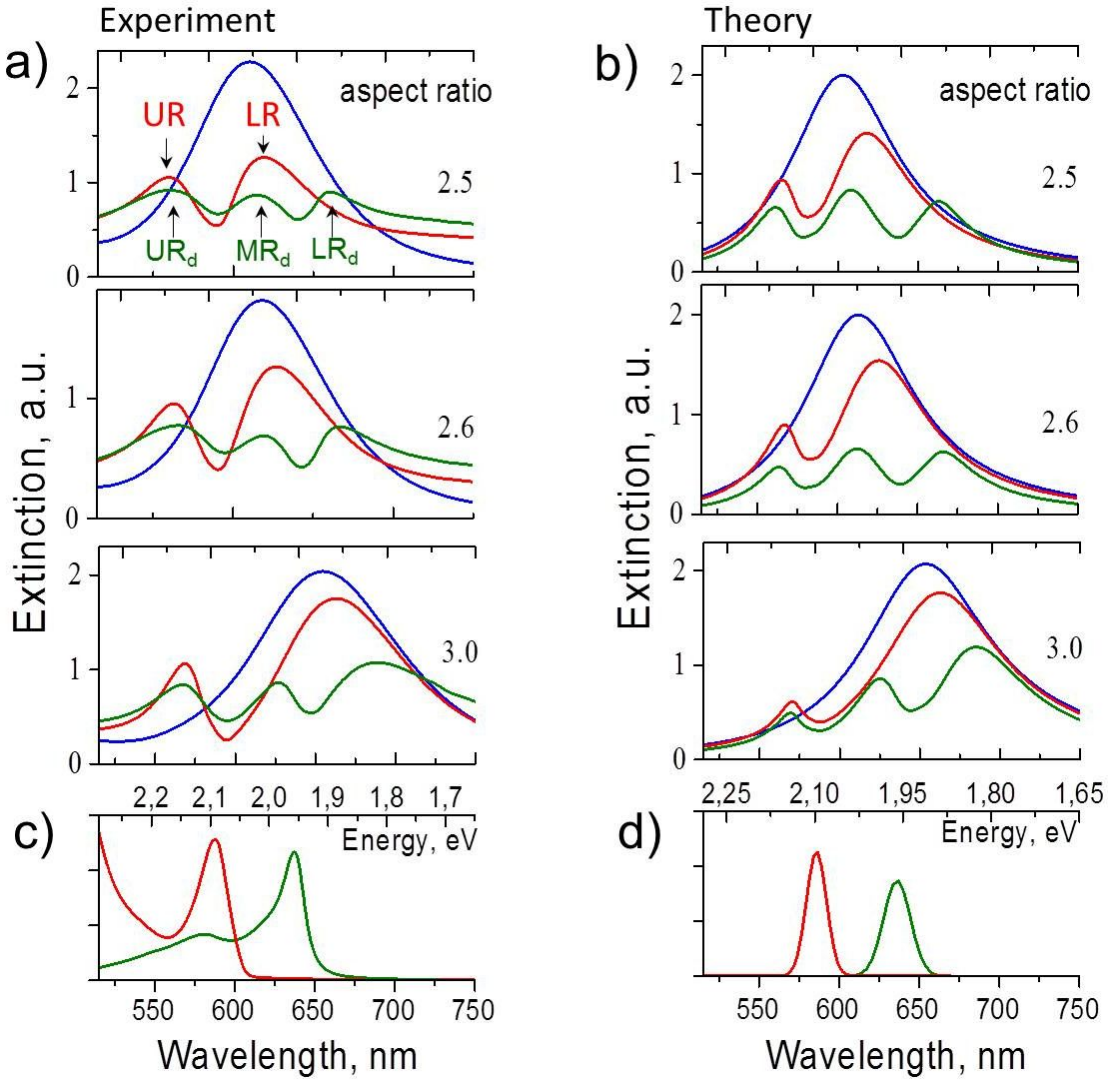

Figure 2. Experimental (a) and theoretical (b) extinction spectra of aqueous dispersions of bare core-shell Au@Ag NRs (blue), the hybrid system of J-aggregates of TCI and Au@Ag NRs (red) and the hybrid structure of J-

aggregates of two fluorophores (TCI and DBI) and Au@Ag NRs, with different aspect ratios. Experimental (c) and theoretical (d) absorption spectra of J-aggregates of TCI (red) and DBI (green) dyes.

As noted above, due to the specific chemical structure and polarity of DBI, J-aggregates of this dye do not form a bound complex with bare Au@Ag NRs, which would show spectral properties related to strong coupling. However, it turned out that the presence of an oppositely charged layer of TCI J-aggregates on the NRs surface triggers the formation of a multilayer hybrid system made of DBI J-aggregates with a NRs/TCI structure (see Methods for more information). We should emphasize that, as indicated in Methods, the simultaneous presence of two separate systems, namely one made of NRs covered only with J-aggregates of DBI, and another of NRs covered with only J-aggregates of TCI, is not possible.

Remarkably, the spectra of this new hybrid complex show double Rabi splitting for all NRs, regardless of their AR, with three plexciton peaks located at 560-567 nm, 614-626 nm and 660-688 nm, respectively, to which we further refer to as upper resonance (URd), medium resonance (MRd) and lower resonance (LRd). In between these plexciton peaks, two pronounced dips are also observed, with minima at 590-595 and 640-647 nm. These dips coincide with the spectral positions of the J-bands of TCI and DBI, but in both cases redshifted by several nanometers relative to the

extinction maxima of J-aggregates. We attribute this effect to a Lamb shift caused by adsorption of J-aggregates on the NRs surface [4].

As shown in Figure 2b, the lineshapes in the spectra of both NRs/TCI and NRs/TCI/DBI structures for NRs with different ARs are properly described by the theoretical model (see details in the Supporting Information, SI), which takes into account the coating of gold NRs with two layers of J-aggregates of different dyes.

The dips observed in the spectra of the hybrid plasmon-exciton structure are due to the formation of two distinct hybridized states (plexcitons), which leads to Rabi splitting in optical spectra [4, 7]. To sum up the data on exciton-plasmon coupling in the system of Au@Ag NRs with different aspect ratios and TBI and DBI J-aggregates, we plotted the spectral position of the hybridized plexciton states as a function of the position of the plasmon peak in the spectra of bare NRs for the case of single (Figure 3a) and double Rabi splitting (Figure 3b). Correlating the theoretical and experimental data obtained for the NRs/TCI hybrid structure (Figure 3a), we revealed an anti-crossing effect as a result of the strong coupling between the NRs plasmon and the exciton of J-aggregates, which leads to a considerably large Rabi splitting $\hbar\Omega_R \approx 175$ meV. The value of Ω_R was

evaluated as the difference between the UR and LR energies at zero detuning (intersection of dashed lines in Figure 3a) by fitting the theoretical model, adopted from Ref.[26] (solid lines in Fig.3a,b) and described in SI, to the experimental data.

Figure 3c gives a simple schematic representation of the energy states in the NRs/TCI hybrid structure with a single Rabi splitting, which demonstrates the hybridization of electronic states due to the strong coupling of exciton states and the plasmon LR of a metal nanostructure. Obviously, in the case of a system with double Rabi splitting, the energy state diagram is somewhat more complicated. Figure 3d illustrates the formation of hybridized plexciton states caused by the strong coupling between Au@Ag NRs plasmon and excitons of TCI and DBI J-aggregates, leading to a double Rabi splitting and the appearance of three resonance peaks: UR_d, MR_d and LR_d associated with the corresponding plexitons (green spectra in Fig.2).

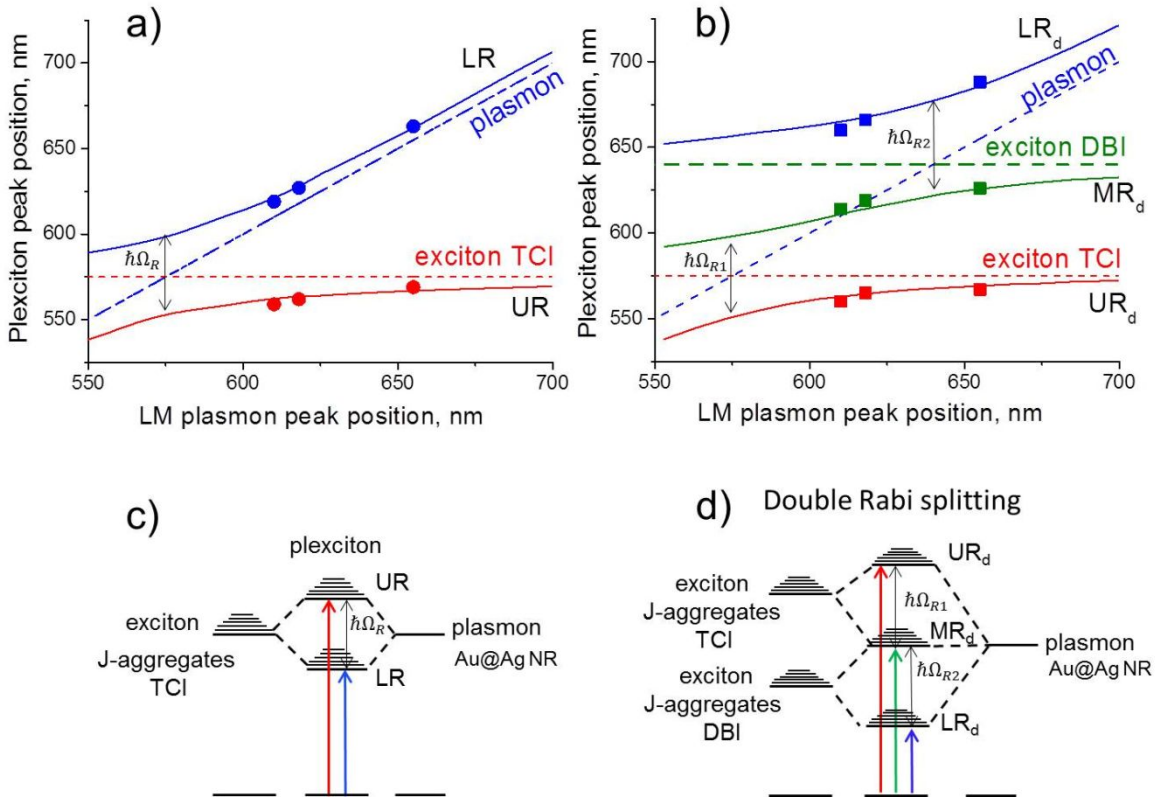

Figure 3. (a) Positions of LR (blue circles) and UR (red circles) in the experimental extinction spectra of the hybrid structure of Au@Ag NRs and TCI J-aggregates dye, as a function of the plasmon peak position in the spectra of bare NRs. (b) Positions of LRd (blue squares), MRd (green squares) and URd (red circles) in the experimental extinction spectra of the hybrid structure of Au@Ag NRs and J-aggregates of TCI and DBI dyes with double Rabi splitting, as a function of the plasmon peak position in the spectra of bare NRs. The blue, green and red solid curves show the theoretically calculated spectral positions of LR_d, MR_d and UR_d, respectively. The horizontal red and green dashed lines indicate

the spectral position of the J-band of TCI and DBI, respectively. The diagonal blue dashed lines mark the position of the plasmon resonance. (c) Schematic representation of the strong coupling between the J-aggregates exciton (left) and the NRs plasmon (right), yielding two hybrid plexciton states. (d) Schematic representation of the strong coupling between the excitons of the J-aggregates of TCI and DBI (left) and the plasmon of Au@Ag NRs (right), yielding three hybridized plexciton states and double Rabi splitting.

For NRs/TCI structures with different ARs, LR peaks are located both to the right and to the left of the DBI J-band, which allows us to reveal more clearly the spectral behavior of plexcitons in the case of double Rabi splitting. For NRs with a higher AR, namely 3, the J-band is located is to the right of the LR of the NRs/TCI hybrid structure, and therefore the spectral position of the LR_d (blue dots) approaches the position of the plasmon peak of bare NRs (dotted blue line), while the MR_d (green dots) tends to the position of the DBI aggregate exciton (dotted green line). However, for NRs with the smallest AR (2.5), the J-band is located to the left of the LR of the NRs/TCI hybrid structure, and the spectral behavior of the plexciton states is completely different. Now, the LR_d (blue dots)

tends to the position of the DBI J-aggregate exciton (dotted green line), while the MRd (green dots) cross the spectral position of the longitudinal LSPR (dotted blue line) and approach the LR plexciton state of the NRs/TCI hybrid structure.

Figure 3b also shows the theoretical results (solid lines, see SI for modeling details) for Ag@Au NRs with two J-aggregates fitted to the experimental data obtained for the hybrid plexiton states in the case of double Rabi splitting. Using this model to interpolate/extrapolate the experimental data (symbols in Figure 3b) to zero detuning allows for estimating the Rabi splitting values to be $\hbar\Omega_{R1} \approx$ 175 and $\hbar\Omega_{R2} \approx 163$ meV. These values of Rabi splitting for the Au@Ag/TCI/DBI hybrid structures are comparable to the data reported for two different J-aggregated molecular dyes incorporated in a microcavity [2]. Moreover, in our system, where all three components are involved in the strong interaction in a concerted manner, the total value of 338 meV reflects the onset of collective extended energy splitting between the states of the lower and upper plexitons (Figure 3b,d).

Another striking result of this study is the detection of a strong magneto-optical (MO) activity of the collectively interacting three-component exciton-plasmon

system. It has been shown that the metal nanoparticles themselves possess MO activity [27]. It was intriguing to check whether all three components of the system show the MO response when interacting in the strong coupling regime. If so, this will be another proof that all components of the system are strongly coupled to each other, working in unison.

To get a deeper insight in this issue, the MO properties of Au@Ag NRs, integrated with the J-aggregates of two different dyes, were studied. In these experiments, magnetic circular dichroism (MCD) spectra (the difference between the absorbance of left- and right-hand polarized light, $\Delta A(\lambda)$, under an applied magnetic field) were recorded for all samples. The results are plotted in Figure 4.

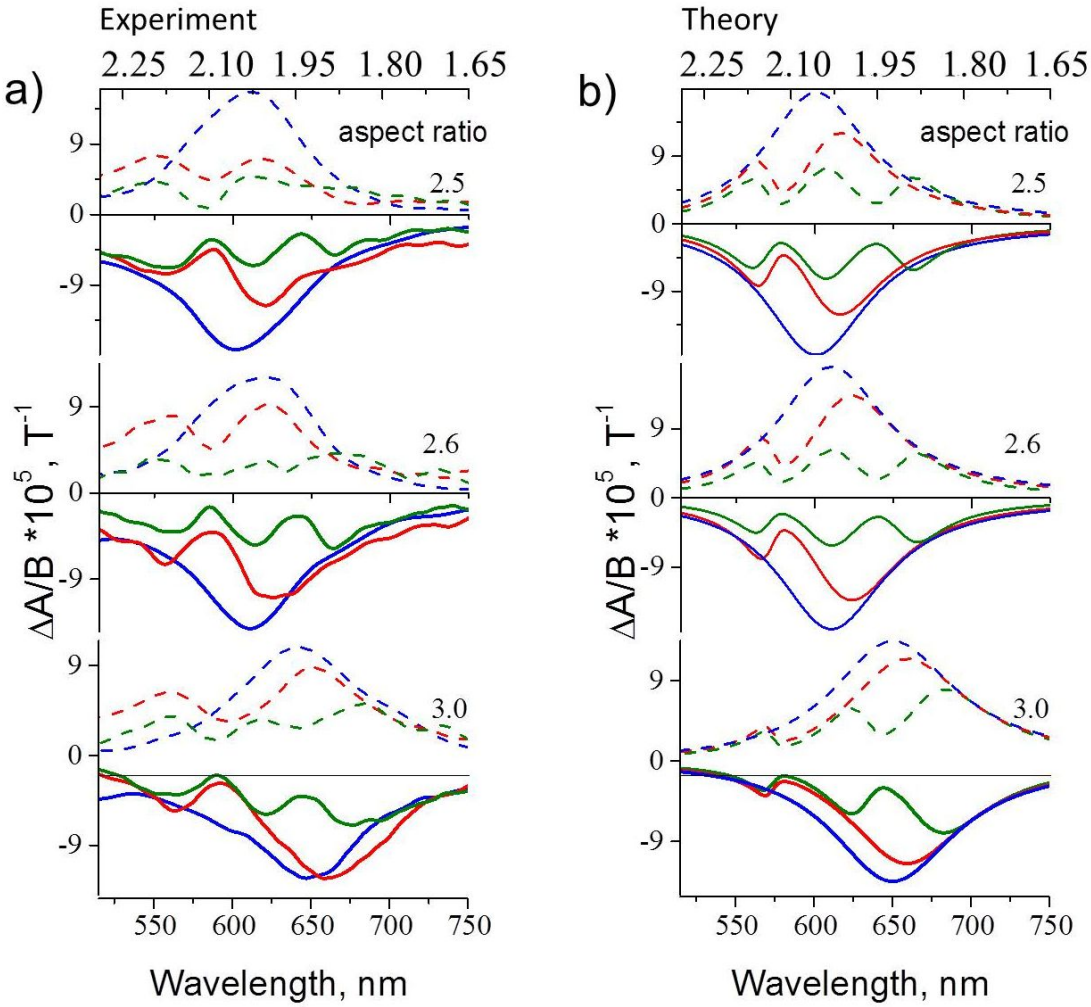

Figure 4. Experimental (a) and theoretical (b) spectra of (i) MCD of Au@Ag NRs with different aspect ratios (blue line), (ii) hybrid structure consisting of Au@Ag NRs and TCI J-aggregates (red line) and (iii) hybrid structures of Au@Ag/TCI/DBI (green line). The MCD spectra were obtained by applying magnetic fields B= 1T (solid lines) and B= -1T (dashed lines).

First, in our experiments a strong MO response was found for bare Au@Ag NRs with different ARs and for the hybrid structures of Au@Ag/TCI J-aggregates (Figure 3, blue and red curves, respectively), which is consistent with previous reports [7, 28-30]. A change in the polarity of the magnetic field leads to a sign reversal

for all MCD spectra. The magnetic properties of plasmonic nanoparticles can be described by a simple model that considers the circular motion of free electrons inside nanoparticles caused by the Lorentz force under the influence of an external magnetic field, with a cyclotron frequency proportional to the magnetic field [31-32]. As a result of this effect, in the case of bare Au@Ag NRs, the application of a magnetic field leads to different absorption for the left- and right-hand circular polarized light, resulting in a rather strong MCD signal. The MO response of the hybrid structures of Au@Ag/TCI J-aggregates arises from the strong plasmon-exciton coupling, as described in detail in our previous work [7].

For the hybrid NRs/TCI/DBI structures, the MCD spectral features correlate well with those in the absorption spectra of the system constituents and for each NRs AR show three distinct peaks in the spectral regions of UR_d (around 550-565 nm), MR_d (around 610-622 nm) and LR_d (664-688 nm). The reversal of the MCD sign of all the peaks of the hybrid NRs/TCI/DBI structure in the MCD spectra observed for the opposite polarity of the magnetic field (Figure 3, dashed lines) clearly demonstrates the magnetic nature of these peaks. It is of paramount importance that the J-aggregates of both TCI and DBI dyes themselves do not exhibit any

pronounced magnetic properties in region of the J-band (SI Figure S1). Nonvanishing MCD signal near the TCI and DBI excitons is the ultimate verification of the strong coupling in the system and unambiguously indicates that the plexitons of two different J-aggregates acquire magnetooptical activity due to coupling to the plasmonic nanostructure. The MCD spectra, normalized at the extinction maximum $A_{\max}$ for NRs with AR 3, are presented in Figure S2 and show that MO ($\Delta A/A_{max}$) for three plexciton states of the hybrid NRs/TCI/DBI structure have similar values and are comparable in magnitude to MO of bare NRs. This comparable strength of MO actively confirms our conclusion of the strong coupling regime of interaction.

In summary, we have shown that all components of a hybrid NR/J-aggregate system are involved in strong interactions in a concerted manner, so that strong coupling between a plasmon and two excitons of J-aggregates of different dyes in multi-layer nanostructures, can lead to double Rabi splitting, significantly expanding the region of energy splitting between the states of plexcitons. All presented experimental results, supported by theoretical modeling, convincingly demonstrate a remarkably strong interaction of J-aggregates of two dyes and the plasmon system in the developed structures.

Exciton-plasmon strong coupling in a complex system consisting of two layers of J-aggregates of different dyes on Au@Ag NRs surface, is confirmed not only by theoretical modeling, but also by the results of MO activity in the same hybrid structures, which is the ultimate verification of the strong coupling in the system for each type of excitons. The manifestation of pronounced magnetic properties for the three plexciton states indicates that the plexitons of J-aggregates of two non-magnetic dyes effectively acquire “magnetic” properties from the plasmonic nanostructure, as a result of interactions in the strong coupling regime. Since in such a system, all hybrid plexciton states exhibit magneto-optical activity, MO can be used to study the fundamental properties of hybrid organic/inorganic systems in the strong coupling regime, which may also have great implications for biosensing, which is intrinsically insensitive to the organic background and thus offers a significant advantage over conventional spectroscopy methods. The development of a multi-component system with extended Rabi splitting represents a new paradigm for various applications even beyond sensing and opens up ample opportunities for research of multimode hybridization and fast and effective energy transfer between two excitons strongly coupled to plasmonic nanostructures.

METHODS

Cyanine dye 5,5′,6,6′-Tetrachloro-1,1′,3,3′-tetraethyl-imidacarbocyanine iodide, tetrachloroauric acid ($HAuCl_4$), sodium borohydride ($NaBH_4$), CTAB, BDAC, silver nitrate ($AgNO_3$), hydrochloric acid (HCl) and ascorbic acid (AA) were purchased from Sigma-Aldrich. Fluorophore 2-[3-[1,1-dimethyl-3-(4-sulfobutyl)-1,3-dihydro-benzo[e]indol-2-ylidene]-propenyl]-1,1-dimethyl-3-(4-sulfobutyl)-1H-benzo[e]indolium hydroxide, inner salt, sodium salt S 2165 was obtained from FEW Chemicals.

Gold NRs were prepared using Ag-assisted seeded growth [33]. Seeds were prepared by the reduction of $HAuCl_4$ (5 mL, 0.25 mM) with $NaBH_4$ (0.3 mL, 10 mM) in aqueous CTAB solution (100 mM). An aliquot of seed solution (0.12 mL) was added to a growth solution containing CTAB (50 mL, 100 mM), $HAuCl_4$ (0.5 mL, 50 mM), ascorbic acid (0.4 mL, 100 mM), $AgNO_3$ (0.6 mL, 10 mM) and HCl (0.95 mL, 1000 mM). The mixture was left undisturbed at 30 ºC for 2 h. The solution was centrifuged twice (8000 rpm, 30 min) and redispersed in BDAC (10 mM) to obtain a final concentration of gold equal to 0.25 mM. The maximum of LSPR band of initially obtained gold NRs was 860 nm.

Core-shell Au@Ag NRs were synthesized using benzyldimethylhexadecylammonium chloride (BDAC) as the capping agent [25]. The typical reaction involved the addition of different amounts of $AgNO_3$ (10 mM) and ascorbic acid (100 mM) to the solution of gold NRs (10 mL, 0.25 mM) at 60 ºC. Larger amounts of silver caused more pronounced LSPR blue shifts. Addition of 1.0 mL, 0.9 mL, or 0.8 mL of $AgNO_3$ (10 mM), while maintaining the molar ratio of Ascorbic Acid to Ag^+ equal to 4, enabled us to reach LSPR maxima at 609 nm, 618 nm, or 655 nm, respectively. The solutions were left for 3 hours at 60 ºC under magnetic stirring. Finally, the solutions were centrifuged twice (6000-9000 rpm, 40 min) and redispersed in BDAC (2 mL, 15 mM).

J-aggregates of the TCI dye were formed spontaneously upon dissolution of this dye in aqueous NaOH or NH_3 solution (pH=8) [16, 34], while the formation of J-aggregates of DBI dye required addition of a positively charged polyelectrolyte, such as PEI, PDDA, or BDAC.

Hybrid structures of Au@Ag NRs and J-aggregates of TCI dye were obtained by addition of 10 µL of a concentrated ethanol solution of dye to 1 mL of an aqueous solution of NRs in the presence of ammonia (pH=8), followed by gentle

stirring for 20 minutes. To separate J-aggregates bound to NRs from monomer dye molecules and free J-aggregates, the solution was centrifuged at 3500 rpm for 5 minutes and redispersed in water. Despite the fact that the concentration of the stabilizing agent BDAC is significantly reduced after centrifugation, the layer of TCI J-aggregates on the surface of Au@Ag NRs protects them from aggregation, thus providing a stable colloidal dispersion.

To form the hybrid system of Au@Ag NRs and J-aggregates of two different fluorophores, we used the electrostatic interaction between cationic groups of TCI and anionic groups of DBI dyes. In this procedure 3 μL of a concentrated aqueous solution of DBI dye was added to the previously prepared solution of hybrid structures of Au@Ag NRs and TCI J-aggregates followed by gently stirring the solution for 5-10 minutes. In turn, the presence of hybrid structures of Au@Ag/TCI J-aggregates in solution triggers the formation of J-aggregates of DBI dye.

Optical extinction spectra were measured using a Cary 50 spectrometer (Agilent Technologies). Transmission electron microscopy (TEM) images of NRs were obtained using a transmission electron microscope FEG-TEM, JEOL JEM-2100F UHR. For MCD experiments, a Jasco J-815 spectropolarimeter equipped

with a water cooled GMW 3470 electromagnet (providing a static magnetic field of up to 1 T) was used.

The total value of magnetic circular dichroism was calculated as $\Delta A_0 = \theta/\left(\frac{\ln 10}{4}\right)$, where θ is the measured ellipticity, ΔA_0 is the sum of CD due to molecular symmetry and MCD induced by the magnetic field. In this case, the CD was measured as the signal at zero magnetic field (B), which was then subtracted from ΔA_0, yielding the MCD (ΔA) – the difference in absorbance between the right and the left hand polarized light induced by an external magnetic field [35]. ΔA depends on the absorbent concentration and can be expressed as: $\Delta A = \Delta\varepsilon_M c l$ [36], where l is the optical path length through the sample, c is the molar concentration, and $\Delta\varepsilon_M$ is the differential molar extinction. To correctly compare the MCD response in samples of different concentrations, the MCD signals were normalized at the absorption maximum$A_{\max}$, according to$\Delta A(\lambda)/(A_{\max} B) \propto \Delta\varepsilon_M$, where $A_{\max}$ is the absorption maximum for the particular sample. Such a normalization essentially yields the intrinsic MCD parameter$\Delta\varepsilon_M$. In this work, we consider the extinction spectra measured by our spectrometer as absorption

spectra due to the weak light scattering by the used samples. All experiments were performed in ambient atmosphere at room temperature.

Theoretical calculations were performed using the tensorial model developed in Ref. 26. According to it, the nanorods were represented as several concentric spheroidal shells with the dielectric properties corresponding to Ag, Au and J-aggregated dyes and the experimental aspect ratios. Self-consistent solution of Maxwell's equations in each shell returns the effective dielectric tensor for the solution of particles dispersed in the host medium from which the absorption and the MCD signals can be calculated (see full details in the Supporting Information).

ASSOCIATED CONTENT

The following files are available free of charge: (PDF)

Calculation of the absorption and MCD spectra for a nanorods solution coupled with J-aggregates. Absorption and MCD spectra pure TCI J-aggregates pure DBI J-aggregates (green line). Experimental and theoretical extinction and MCD spectra of core-shell Au@Ag NRs, hybrid core-shell Au@Ag/J-aggregates TCI structure and hybrid structure of core-shell Au@Ag/TCI/DBI NRs.

AUTHOR INFORMATION

Corresponding Author

*Yury.Rakovich@ehu.eus

ACKNOWLEDGMENT

This work was supported by MINECO (Ministerio de Economiá y Competitividad), Spain, project Fis2016.80174-P (PLASMOQUANTA) and MAT2017-86659-R (MULTIMAGE). I.N. and Y.R. acknowledge support from the Ministry of Education and Science of the Russian Federation under grant no. 14.Y26.31.0011 and funding from the Basque Government (Grant No. IT1164-19). This work was coordinated under the Maria de Maeztu Units of Excellence Program from the Spanish State Research Agency (Grant No. MDM-2017-0720).

REFERENCES

(1) Hutchison, J. A.; Schwartz, T.; Genet, C.; Devaux, E.; Ebbesen, T. W. Modifying Chemical Landscapes by Coupling to Vacuum Fields. *Angew. Chem. Int. Ed.* **2012,** *51*, 1592–1596.

(2) Coles, D. M.; Somaschi, N.; Michetti, P.; Clark, C.; Lagoudakis, P. G.; Savvidis, P. G.; Lidzey, D. G. Polariton-mediated energy transfer between

organic dyes in a strongly coupled optical microcavity. *Nat. Mater.* **2014,** *13*, 712–719.

(3) Wiederrecht, G. P.; Hall, J. E.; Bouhelier, A. Control of Molecular Energy Redistribution Pathways via Surface Plasmon Gating. *Phys. Rev. Lett.* **2007,** *98*, 083001.

(4) Melnikau, D.; Esteban, R.; Savateeva, D.; Sánchez-Iglesias, A.; Grzelczak, M.; Schmidt, M. K.; Liz-Marzán, L. M.; Aizpurua, J.; Rakovich, Y. P. Rabi Splitting in Photoluminescence Spectra of Hybrid Systems of Gold Nanorods and J-Aggregates. *J. Phys. Chem. Lett.* **2016,** *7*, 354-362.

(5) Dong, Z. C.; Zhang, X. L.; Gao, H. Y.; Luo, Y.; Zhang, C.; Chen, L. G.; Zhang, R.; Tao, X.; Zhang, Y.; Yang, J. L.; Hou, J. G. Generation of molecular hot electroluminescence by resonant nanocavity plasmons. *Nat. Photon.* **2010,** *4*, 50–54.

(6) Orgiu, E.; George, J.; Hutchison, J. A.; Devaux, E.; Dayen, J. F.; Doudin, B.; Stellacci, F.; Genet, C.; Schachenmayer, J.; Genes, C.; Pupillo, G.; Samori, P.; Ebbesen, T. W. Conductivity in organic semiconductors hybridized with the vacuum field. *Nat. Mater.* **2015,** *14*, 1123-1129.

(7) Melnikau, D.; Govyadinov, A. A.; Sánchez-Iglesias, A.; Grzelczak, M.; Liz-Marzán, L. M.; Rakovich, Y. P. Strong Magneto-Optical Response of Nonmagnetic Organic Materials Coupled to Plasmonic Nanostructures. *Nano Lett.* **2017,** *17*, 1808-1813.

(8) Wiederrecht, G. P.; Wurtz, G. A.; Hranisavljevic, J. Coherent Coupling of Molecular Excitons to Electronic Polarizations of Noble Metal Nanoparticles. *Nano Lett.* **2004,** *4*, 2121–2125.

(9) Kurizki, G.; Bertet, P.; Kubo, Y.; Molmer, K.; Petrosyan, D.; Rabl, P.; Schmiedmayer, J. Quantum technologies with hybrid systems. *Proc. Natl. Acad. Sci. USA* **2015,** *112*, 3866–3873.

(10) Reithmaier, J. P.; Sek, G.; Loffler, A.; Hofmann, C.; Kuhn, S.; Reitzenstein, S.; Keldysh, L. V.; Kulakovskii, V. D.; Reinecke, T. L.; Forchel, A. Strong coupling in a single quantum dot-semiconductor microcavity system. *Nature* **2004,** *432*, 197-200.

(11) Hennessy, K.; Badolato, A.; Winger, M.; Gerace, D.; Atature, M.; Gulde, S.; Falt, S.; Hu, E. L.; Imamoglu, A. Quantum nature of a strongly coupled single quantum dot-cavity system. *Nature* **2007,** *445*, 896-899.

(12) Ming, T.; Zhao, L.; Xiao, M.; Wang, J. Resonance-Coupling-Based Plasmonic Switches. *Small* **2010,** *6*, 2514–2519.

(13) Hakala, T. K.; Toppari, J. J.; Kuzyk, A.; Pettersson, M.; Tikkanen, H.; Kunttu, H.; Torma, P. Vacuum Rabi Splitting and Strong-Coupling Dynamics for Surface-Plasmon Polaritons and Rhodamine 6G Molecules. *Phys. Rev. Lett.* **2009,** *103*, 053602–4.

(14) Wang, H.; Wang, H.-Y.; Wang, L.; Chen, Q.-D.; Xu, H.-L.; Carrara, A.; Proietti Zaccaria, R.; Sun, H.-B.; Toma, A. Multimode Coherent Hybrid States: Ultrafast Investigation of Double Rabi Splitting between Surface Plasmons and Sulforhodamine 101 Dyes. *Adv. Opt. Mater.* **2017,** *5*, 1600857.

(15) George, J.; Chervy, T.; Shalabney, A.; Devaux, E.; Hiura, H.; Genet, C.; Ebbesen, T. W. Multiple Rabi Splittings under Ultrastrong Vibrational Coupling. *Phys. Rev. Lett.* **2016,** *117*, 153601.

(16) Melnikau, D.; Savateeva, D.; Susha, A. S.; Rogach, A. L.; Rakovich, Y. P. Strong plasmon-exciton coupling in a hybrid system of gold nanostars and J-aggregates. *Nanoscale Res. Lett.* **2013,** *8*, 134.

(17) Hensen, M.; Heilpern, T.; Gray, S. K.; Pfeiffer, W. Strong Coupling and Entanglement of Quantum Emitters Embedded in a Nanoantenna-Enhanced Plasmonic Cavity. *ACS Photonics* **2017,** *5*, 240-248.

(18) Hartmann, M. J. Quantum simulation with interacting photons. *J. Opt.* **2016,** *18*, 104005.

(19) Dovzhenko, D. S.; Ryabchuk, S. V.; Rakovich, Y. P.; Nabiev, I. R. Light-matter interaction in the strong coupling regime: configurations, conditions, and applications. *Nanoscale* **2018,** *10*, 3589-3605.

(20) Cuadra, J.; Baranov, D. G.; Wersäll, M.; Verre, R.; Antosiewicz, T. J.; Shegai, T. Observation of Tunable Charged Exciton Polaritons in Hybrid Monolayer WS2−Plasmonic Nanoantenna System. *Nano Lett.* **2018,** *18*, 1777-1785.

(21) Kirstein, S.; Daehne, S. J-aggregates of amphiphilic cyanine dyes: Self-organization of artificial light harvesting complexes. *Int. J. Photoenergy* **2006,** *2006*, ID 20363.

(22) Novo, C.; Gomez, D.; Perez-Juste, J.; Zhang, Z.; Petrova, H.; Reismann, M.; Mulvaney, P.; Hartland, G. V. Contributions from radiation

damping and surface scattering to the linewidth of the longitudinal plasmon band of gold nanorods: a single particle study. *Phys. Chem. Chem. Phys.* **2006,** *8*, 3540-3546.

(23) Muskens, O. L.; Bachelier, G.; Fatti, N. D.; Vallée, F.; Brioude, A.; Jiang, X.; Pileni, M.-P. Quantitative Absorption Spectroscopy of a Single Gold Nanorod. *The Journal of Physical Chemistry C* **2008,** *112*, 8917-8921.

(24) Heylman, K. D.; Thakkar, N.; Horak, E. H.; Quillin, S. C.; Cherqui, C.; Knapper, K. A.; Masiello, D. J.; Goldsmith, R. H. Optical microresonators as single-particle absorption spectrometers. *Nat. Photon.* **2016,** *10*, 788-795.

(25) Gómez-Graña, S.; Goris, B.; Altantzis, T.; Fernández-López, C.; Carbó-Argibay, E.; Guerrero-Martínez, A.; Almora-Barrios, N.; López, N.; Pastoriza-Santos, I.; Pérez-Juste, J.; Bals, S.; Van Tendeloo, G.; Liz-Marzán, L. M. Au@Ag Nanoparticles: Halides Stabilize {100} Facets. *J. Phys. Chem. Lett.* **2013,** *4*, 2209-2216.

(26) Abe, M.; Suwa, T. Surface plasma resonance and magneto-optical enhancement in composites containing multicore-shell structured nanoparticles. *Phys. Rev. B* **2004,** *70*, 235103.

(27) Pineider, F.; Campo, G.; Bonanni, V.; Fernández, C. d. J.; Mattei, G.; Caneschi, A.; Gatteschi, D.; Sangregorio, C. Circular Magnetoplasmonic Modes in Gold Nanoparticles. *Nano Lett.* **2013,** *13*, 4785–4789.

(28) Sepúlveda, B.; Calle, A.; Lechuga, L. M.; Armelles, G. Highly sensitive detection of biomolecules with the magneto-optic surface-plasmon-resonance sensor. *Opt. Lett.* **2006,** *31*, 1085-1087.

(29) Pineider, F.; Campo, G.; Bonanni, V.; Fernandez, C. J.; Mattei, G.; Caneschi, A.; Gatteschi, D.; Sangregorio, C. Circular Magnetoplasmonic Modes in Gold Nanoparticles. *Nano letters* **2013,** *13*, 4785-4789.

(30) Artemyev, M.; Krutokhvostov, R.; Melnikau, D.; Oleinikov, V.; Sukhanova, A.; Nabiev, I. Low-field magnetic circular dichroism in silver and gold colloidal nanoparticles of different sizes, shapes, and aggregation states. *Proc Spie* **2012,** *8457*.

(31) Armelles, G.; Cebollada, A.; Garcia-Martin, A.; Gonzalez, M. U. Magnetoplasmonics: Combining Magnetic and Plasmonic Functionalities. *Adv Opt Mater* **2013,** *1*, 10-35.

(32) Fan, S. Magnet-controlled plasmons. *Nat. Photon.* **2010,** *4*, 76.

(33) Liu, M. Z.; Guyot-Sionnest, P. Mechanism of silver(I)-assisted growth of gold nanorods and bipyramids. *J Phys Chem B* **2005,** *109*, 22192-22200.

(34) Melnikau, D.; Savateeva, D.; Susha, A.; Rogach, A. L.; Rakovich, Y. P. Strong plasmon-exciton coupling in a hybrid system of gold nanostars and J-aggregates. *Nanoscale Res. Lett.* **2013,** *8*.

(35) Sutherland, J. C.; Holmquist, B. Magnetic Circular-Dichroism of Biological Molecules. *Annu Rev Biophys Bio* **1980,** *9*, 293-326.

(36) Mason, W. R. *A practical guide to magnetic circular dichroism spectroscopy*. Wiley-Interscience: Hoboken, N.J., 2007; p xii, 223 p.

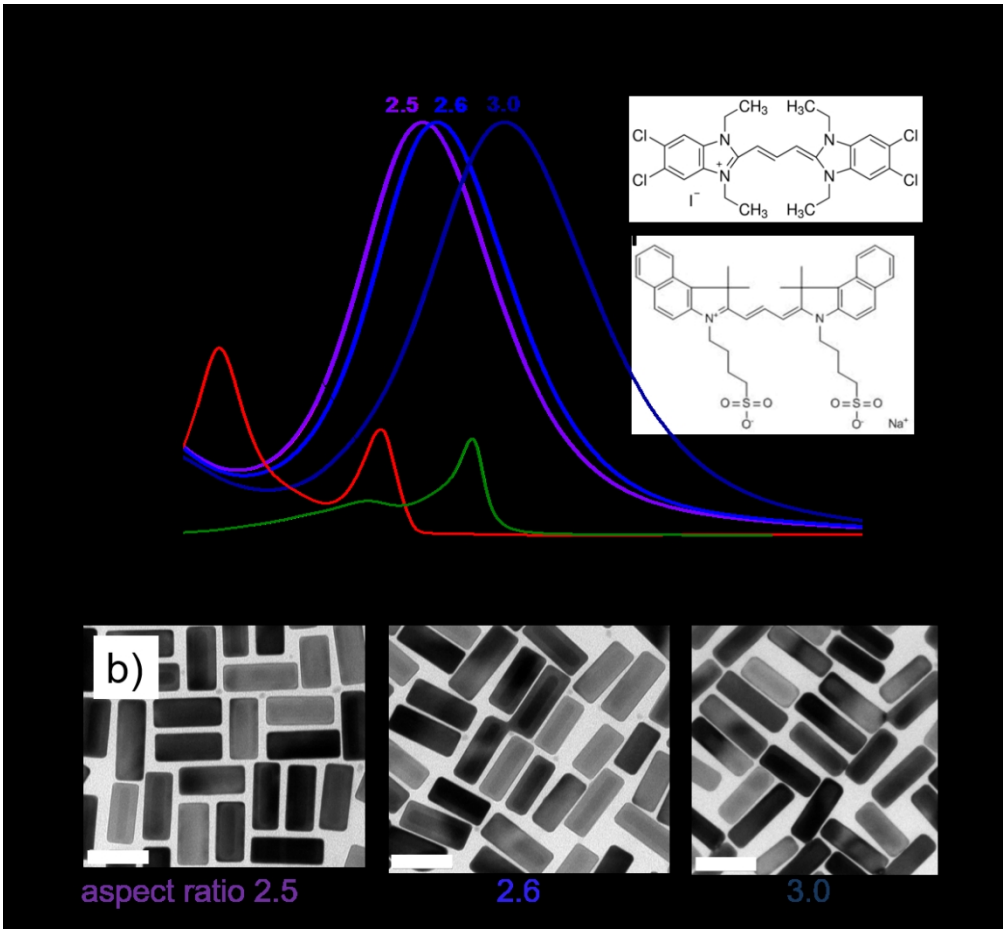

Figure 1. (a) Experimental extinction spectra of an aqueous dispersion of core-shell Au@Ag NRs of different aspect ratios (2.5 – 3.0) and absorption spectra of J-aggregates of TCI and DBI fluorophores (inset: chemical structures of TCI and DBI fluorophores). (b) TEM images of core-shell Au@Ag NRs with average aspect ratios varying from 2.5 to 3; scale bars are 50 nm.

200x185mm (150 x 150 DPI)

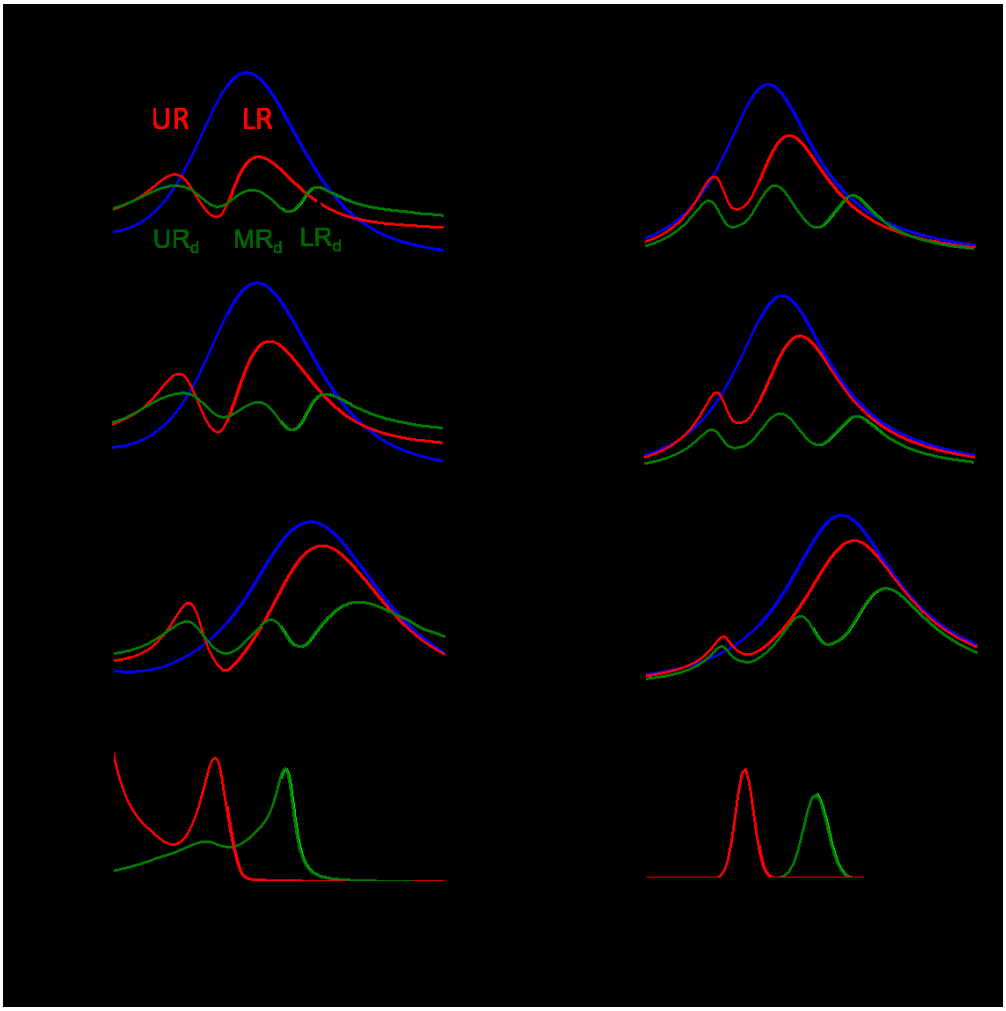

Figure 2. Experimental (a) and theoretical (b) extinction spectra of aqueous dispersions of bare core-shell Au@Ag NRs (blue), the hybrid system of J-aggregates of TCI and Au@Ag NRs (red) and the hybrid structure of J-aggregates of two fluorophores (TCI and DBI) and Au@Ag NRs, with different aspect ratios. Experimental (c) and theoretical (d) absorption spectra of J-aggregates of TCI (red) and DBI (green) dyes.

192x192mm (150 x 150 DPI)

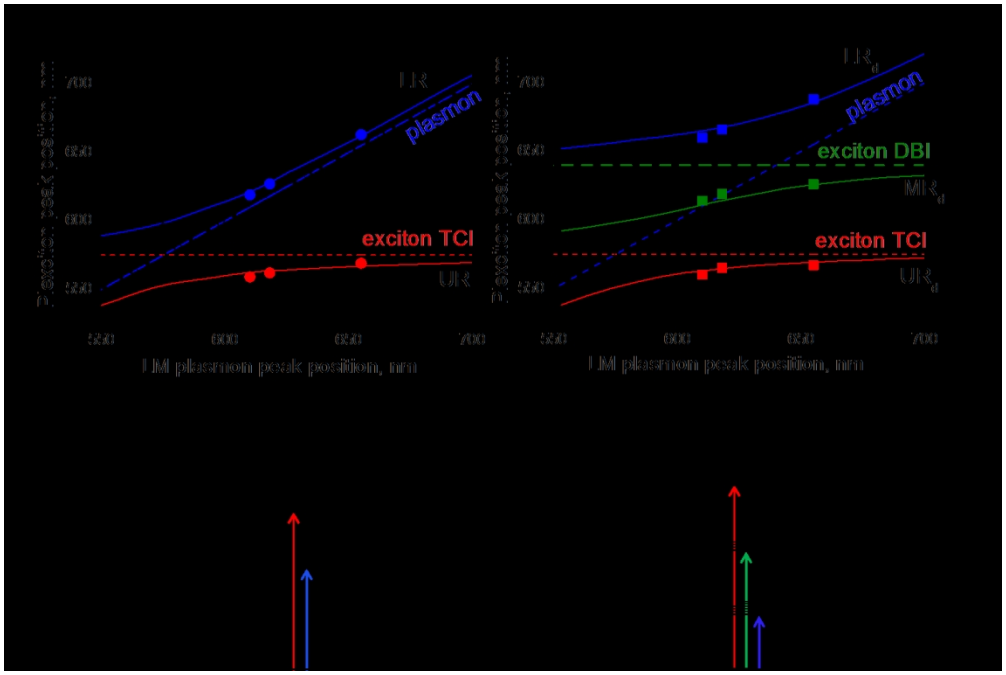

Figure 3. (a) Positions of LR (blue circles) and UR (red circles) in the experimental extinction spectra of the hybrid structure of Au@Ag NRs and TCI J-aggregates dye, as a function of the plasmon peak position in the spectra of bare NRs. (b) Positions of LRd (blue squares), MRd (green squares) and URd (red circles) in the experimental extinction spectra of the hybrid structure of Au@Ag NRs and J-aggregates of TCI and DBI dyes with double Rabi splitting, as a function of the plasmon peak position in the spectra of bare NRs. The blue, green and red solid curves show the theoretically calculated spectral positions of LRd, MRd and URd, respectively. The horizontal red and green dashed lines indicate the spectral position of the J-band of TCI and DBI, respectively. The diagonal blue dashed lines mark the position of the plasmon resonance. (c) Schematic representation of the strong coupling between the J-aggregates exciton (left) and the NRs plasmon (right), yielding two hybrid plexciton states. (d) Schematic representation of the strong coupling between the excitons of the J-aggregates of TCI and DBI (left) and the plasmon of Au@Ag NRs (right), yielding three hybridized plexciton states and double Rabi splitting.

261x174mm (150 x 150 DPI)

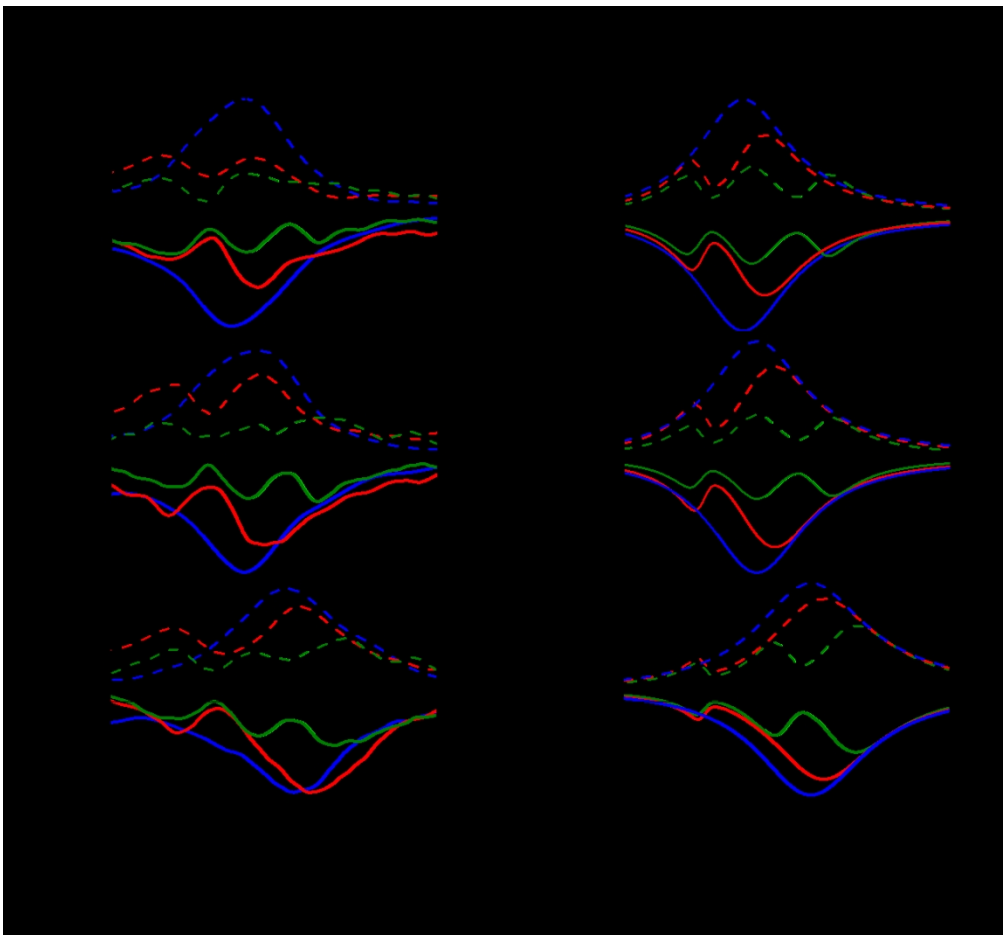

Figure 4. Experimental (a) and theoretical (b) spectra of (i) MCD of Au@Ag NRs with different aspect ratios (blue line), (ii) hybrid structure consisting of Au@Ag NRs and TCI J-aggregates (red line) and (iii) hybrid structures of Au@Ag/TCI/DBI (green line). The MCD spectra were obtained by applying magnetic fields B= 1T (solid lines) and B= -1T (dashed lines).

215x199mm (150 x 150 DPI)